Relationship of Interfacial Equilibria to Interfacial Activation of Phospholipase A_2†

Mahendra Kumar Jain,*,‡ Bao-Zhu Yu,‡ and Otto G. Berg*,§

Department of Chemistry and Biochemistry, University of Delaware, Newark, Delaware 19716, and Department of Molecular Biology, Uppsala University Biomedical Center, Uppsala, Sweden

Received May 27, 1993; Revised Manuscript Received August 9, 1993®

ABSTRACT: The equilibrium dissociation constants for the distribution of pig pancreatic phospholipase A2, its competitive inhibitors, and their complexes at the interface of a neutral diluent are determined. The relationship between these parameters and their significance for interfacial catalysis is elaborated in terms of a model based on the relationship between the underlying equilibria. By using a combination of spectroscopic and chemical modification methods, it was possible to determine the equilibrium dissociation constant of an inhibitor bound to the interface (K') or of the inhibitor bound to the enzyme in the aqueous phase (K_I) or the interface (K_I^*). The equilibrium dissociation constant for the free enzyme (K_d) or for the enzyme–inhibitor complex (K_d^I) from the interface were also obtained. These constants are shown to be thermodynamically related, i.e., $K'K_dK_I^* = K_IK_d^I$, as predicted on the basis of the cyclic equilibrium scheme (thermodynamic box) describing the distribution of the enzyme and the inhibitor between the aqueous phase and the interface at constant calcium concentration. Results show that (i) calcium is required for the binding of a substrate or inhibitor molecule to the catalytic site; (ii) the effective dissociation constant of the inhibitor–enzyme complex in the aqueous phase is considerably larger than that for the enzyme at the interface, i.e., $K_I \gg$ effective K_I^*; (iii) K_d^I does not depend on the structure of the inhibitor and $K_d \gg K_d^I$; and (iv) structure–activity correlations suggest that ionic interactions between a ligand and the interfacial recognition site of the enzyme are important for K', which controls the concentration of the bound inhibitor that the enzyme "sees" in the interface. These observations demonstrate that the binding of the enzyme to the interface and the binding of the inhibitor to the active site of the enzyme at the interface are two distinguishable processes. Therefore, binding of a ligand to the active site of the enzyme promotes binding of the enzyme–inhibitor complex to other amphiphiles and the interface with higher affinity. It is suggested that the primary effect of binding the enzyme to the interface is to increase its intrinsic affinity toward the active-site-directed ligands, i.e., the interfacial activation of PLA2 is of K-type.

An analytical description of the kinetics of interfacial catalysis by phospholipase A_2 (PLA2)[1] in the scooting mode has been achieved in terms of the primary rate constants of the catalytic turnover cycle in the interface (Berg et al., 1991; Jain et al., 1991a). In the highly processive scooting mode, the hydrolysis of vesicles of anionic phospholipids occurs such that the enzyme, the substrate, and the products of hydrolysis remain in the interface and do not exchange with the excess vesicles (Jain et al., 1986a). On the other hand, a complete description of interfacial catalysis in the hopping mode has not been possible because under such conditions the effective rate depends on the exchange of the enzyme between the interface and the aqueous phase, as well as the steps of the catalytic turnover cycle in the interface (Jain & Berg, 1989). Many of these interfacial equilibrium and rate processes have not been characterized; therefore, in such cases the residence time of the enzyme on the substrate interface cannot be established with certainty, nor is it possible to rigorously test the effect of binding of the enzyme to the interface on the primary kinetic parameters of PLA2 and their implications for interfacial activation.

In an attempt to establish the nature of the interfacial processes that control the binding of pig pancreatic PLA2 to micelles of a neutral diluent in the presence of active-site-directed ligands, we have developed an analytical formalism and protocols to determine the underlying interfacial equilibria, which are adequately described by the minimal scheme shown in Figure 1. The analytical expression for the relationship of such equilibria to the experimentally measurable quantities are described in the Appendix. The constants that characterize such equilibria in a mixture of PLA2, neutral diluent, and inhibitor are explicitly considered, experimentally determined, their thermodynamic relationship established, and their significance in the context of the interfacial catalysis and interfacial activation discussed.

MATERIALS AND METHODS

All studies reported in this paper were carried out with PLA2 isolated from the acetone powder of pig pancreas (Niewenhuizen et al., 1974). *p*-Nitrophenacyl bromide was from Sigma. MG-14 was a gift from Professor Michael Gelb (Seattle, WA); RM-2 and RM-3 were kindly provided by Dr. Ronald Magolda (Du Pont Co., Wilmington, DE). Deoxy-LPC and inhibitors of the MJ series were synthesized as described (Jain et al., 1991d). Only the (*R*)-isomers of the inhibitors of the MJ series are active; however, racemates were used, and the concentrations are expressed for racemates. Structures of the competitive inhibitors used in this study are

† This work was supported by grants from Sterling Inc. and PHS (GM29703).

* To whom correspondence should be addressed.

‡ University of Delaware.

§ Uppsala University.

® Abstract published in *Advance ACS Abstracts*, October 1, 1993.

[1] Abbreviations: see Figure 2 for the structures of MG-14, RM-2, RM-3, and inhibitors of the MJ series; deoxy-LPC, 1-hexadecylpropanediol-3-phosphocholine; MJ33, 1-hexadecyl-3-trifluoroethyl-*sn*-glycero-2-phosphomethanol; ND, neutral diluent such as deoxy-LPC used in this study; PLA2, phospholipase A_2 from pig pancreas. Definitions of all the equilibrium parameters are shown in Figure 1 and developed in the Appendix.

0006-2960/93/0432-11319$04.00/0

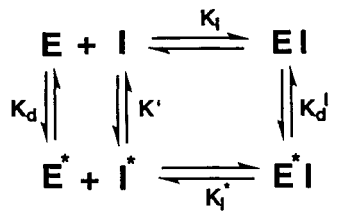

FIGURE 1: Minimal scheme describing the relationships between the various equilibria in a mixture of an enzyme (E), inhibitor (I), and a neutral diluent that forms the interface. A neutral diluent does not bind to the active site of the enzyme, but the free E or its complex with an inhibitor (EI) can bind to the interface of the neutral diluent with dissociation constants K_d and K_d^I, respectively. Similarly, an inhibitor is distributed between the interface and aqueous phase with the distribution coefficient K'. The dissociation constants for EI and E*I are K_I and K_I^*, respectively. For definitions of these equilibria, see the Appendix. Identical schemes hold for other catalytic-site ligands like substrate or product if I is replaced by S or P, respectively.

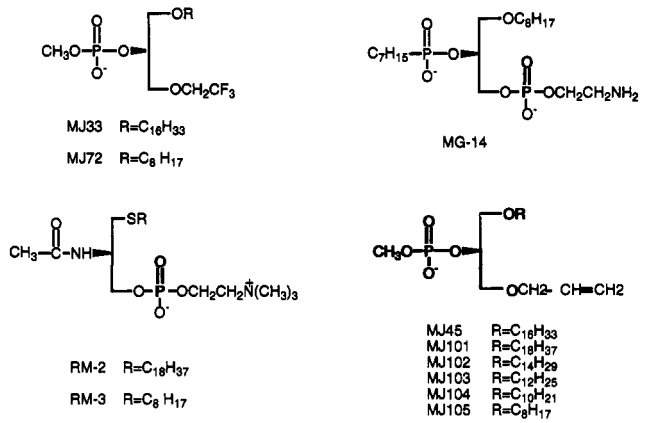

FIGURE 2: Structures of competitive inhibitors used in this paper.

shown in Figure 2, and they were selected for the range of structural diversity and biophysical properties.

Binding to the Active Site. The equilibrium dissociation constant for a ligand bound to the active site of PLA2 was determined by monitoring the rate of alkylation of His-48 by *p*-nitrophenacyl bromide as described elsewhere (Jain et al., 1991a; Yu et al., 1993). Briefly, PLA2 (<1 μM) was incubated at 22 °C in 50 mM cacodylate buffer at pH 7.3 containing human γ-globulin (1 mg/mL), 2 mM *p*-nitrophenacyl bromide, and the active-site-directed ligand at appropriate concentration. For the monitoring of equilibria at the interfaces, the reaction mixtures also contained deoxy-LPC (1.6 mM unless indicated otherwise) as a neutral diluent. At various time intervals, an aliquot of the reaction mixture containing typically 0.1–100 pmol of the enzyme was diluted into an appropriate assay mixture (Jain et al., 1991c; Niewenhuizen et al., 1974; Radvanyi et al., 1989) to measure the residual PLA2 activity. The nonlinear regression of the plot of the residual PLA2 activity as a function of time provided the half-times for inactivation in the absence (t_0) or in the presence (t_L) of a ligand. Since the ligand virtually completely (>95%) protects the active site from alkylation, the effective equilibrium dissociation constant for the ligand, K_L^{eff} (at the saturating concentration of calcium), under a given set of conditions was calculated from the Scrutton–Utter equation as developed and described elsewhere (Jain et al., 1991a).

$$\frac{t_L}{(t_L - t_0)} = 1 + \frac{K_L^{eff}}{[L]} \quad \text{or} \quad \frac{t_L}{t_0} - 1 = \frac{[L]}{K_L^{eff}} \qquad (1)$$

This relationship is based on the fact that the rate of alkylation of the E*L complex is very small (<5%) compared to the rate of alkylation of E*, as shown to be the case (Jain et al., 1991a,d) during the determination of equilibrium dissociation constants for the products (K_P^*), the substrate analogs (K_s^*), and the transition-state mimics (K_I^*).

Binding to the Interface. Binding of PLA2 to micelles of deoxy-LPC was investigated by monitoring the change in the UV absorbance or the fluorescence emission at 333 nm in 20 mM Tris-HCl and 1 mM NaCl at pH 8.0 with 3 mM $CaCl_2$, deoxy-LPC, and other ligands at indicated concentration. The absorbance of PLA2 in the 230–340-nm region was monitored by use of a UV–visible spectrophotometer (Hewlett-Packard 8452) equipped with a diode array detector. The standard software package allowed manipulations that were necessary for obtaining the difference spectra, for corrections due to dilution, and, within certain assumptions, for subtracting the base line due to the light scattering from micelles. The resolution of the spectra were 2 nm; however, spectra were smoothed with a cubic spline function. The resulting difference spectra were similar to those reported by Hille et al. (1983); however, the fine structure of these spectra was found to depend on a variety of factors (Jain & Maliwal, 1993). Typically these measurements were carried out at pH 8.0 with 35 μM PLA2, 3 mM $CaCl_2$, and the indicated amounts of other additives. The first addition was usually of the neutral diluent, and then appropriate amounts of ligands were added in small volumes. This protocol minimized problems due to changes in the light scattering from micelles, and the base line correction was not necessary. Although this protocol was useful for determining K_L^{eff} for PLA2 at the interface of the neutral diluent, it cannot be used to determine the dissociation constant of a ligand bound to PLA2 in the aqueous phase because such interactions do not cause a noticeable characteristic change in the UV absorbance. The change in the absorbance at 292 nm in the presence of an active-site-directed ligand showed concentration dependence and saturation behavior. The concentration dependence could be fitted to a hyperbola to obtain K_L^{eff} (eq A9 or A10 in the Appendix). Since these measurements are made at relatively high enzyme concentrations, it was necessary to make corrections for depletion of the inhibitor (eq A12), especially at low bulk concentrations of the inhibitor. At high concentrations of the neutral diluent when all the enzyme is in the interface, the effective dissociation constant for the inhibitor is given by eq A14 in the Appendix.

Under suitable conditions, it was also possible to obtain the apparent (or effective) dissociation constants by monitoring the fluorescence emission from Trp-3. These measurements were carried out on an SLM 4800S spectrofluorimeter in 20 mM Tris-HCl and 3 mM $CaCl_2$ (unless stated otherwise) at pH 8.0 and 22 °C. The excitation was at 292 nm and the emission at 333 nm, both with slitwidths of 4 nm. For titration curves, the results are expressed as $F/F_0 - 1$, where F_0 is the intensity in the absence of a ligand and F is the intensity in the presence of a ligand. In some experiments, the change in the spectrum in the 300–450-nm region were recorded, and the maximum change in the difference spectrum was always found to be at 333 nm. The PLA2 concentrations for these measurements were typically 2–5 μM; therefore, corrections in the titration curve due to the depletion of the ligand at lower bulk concentrations of the ligand were usually not necessary. Similarly the overall changes in the fluorescence intensity were so large, up to about 250%, that the contributions from dilution and scattering changes were generally negligible. The results, appropriate controls, and corrections described in this paper show that the changes in the fluorescence emission

Table I: Values of Equilibrium Dissociation Constants K_I, K_I^{eff}, K_I^*, and K' for Inhibitors at 23 °C and pH 8.0[a]

inhibitor	K_I (μM)	K_I^{eff} (μM)	K_I^* (mole fraction)	K' (μM)
MJ33(*rac*)	12	1.5	0.0014	<100
MJ72(*rac*)	>90	13	0.0027	<1000
MG14	40	2.3	0.0009	<1000
RM2	>10?	6	0.003	<100
RM3	83	20	0.0033	4000

[a] The K_I^{eff} values were obtained at 1.6 mM deoxy-LPC by the UV absorbance method. K_I^* and K' values were obtained by the protection method (cf. Figure 4).

were due to the formation of the E* and E*I species in the interface. Thus, with titration curves obtained under suitable conditions it was possible to determine appropriate interfacial equilibrium dissociation constants by curve fitting the concentration dependence of the signal. For example, by varying the concentration of the neutral diluent in the absence of a ligand, we obtained K_d, and the corresponding K_d^I values were obtained at saturating inhibitor concentrations. Similarly, by varying the mole fraction of a ligand added to a mixture of PLA2 and saturating neutral diluent (Jain et al., 1991a,d; Yu et al., 1993) it was also possible to obtain K_I, K_I^*, K_P^*, K_S^*, K_{Ca}^*, and K_{Ca} (cf. Figure 1 and its legend for the definition of these dissociation constants) values with an error range of less than 30%. The maximum changes in the fluorescence intensity at 333 nm calculated from such curves are summarized in Table II as F_{EL^*} for the E*L form relative to the value for the enzyme in the aqueous phase (F_E = 1) or the interface (F_{E^*} at 3 mM $CaCl_2$).

RESULTS

The interface of micelles of deoxy-LPC was used for all the measurements of interfacial equilibrium relationships shown in Figure 1. It may be recalled (Jain et al., 1991a,d) that these amphiphiles are neutral diluents, i.e., PLA2 binds to the interface of their micelles, but a neutral diluent molecule does not bind to the active site of the enzyme. The criterion of the protection of His-48 at the catalytic site of PLA2 from alkylation adequately distinguishes a neutral diluent from an active-site-directed ligand. Thus neutral diluents offer a unique opportunity not only to study the properties of the bound enzyme in the absence (E*) or in the presence (E*I) of an inhibitor but also to investigate the equilibria shown in Figure 1.

The binding of a ligand to the active site of PLA2 is most convincingly demonstrated by the protection from alkylation of the catalytic residue His-48 by the active-site-directed ligands such as those shown in Figure 2 (Jain et al., 1991a). For example, as shown in Figure 3, the time course of inactivation of PLA2 by *p*-nitrophenacyl bromide was not noticeably altered in the presence of a neutral diluent such as deoxy-LPC. As also shown in this figure, while MJ72 alone did not protect the active site, the half-time for inactivation increased several-fold in the presence of the inhibitor and deoxy-LPC. From the half-times for alkylation in the presence of varying concentrations of the inhibitor in the presence or absence of the neutral diluent it was possible to obtain values of effective equilibrium dissociation constants for several inhibitors (eq 1). As summarized in Table I, K_I^{eff} values in the presence of a neutral diluent for the short-chain analogues, such as RM-3 and MJ72, were larger than those for the corresponding long-chain analogs RM-2 and MJ33, respectively.

The contribution to K_I^{eff} from a difference in the partition coefficient of the inhibitor between the interface and the aqueous phase was dissected as follows. As developed in the Appendix, the effective equilibrium dissociation constant at a given concentration of the neutral diluent ([ND]) is related to the interfacial equilibrium dissociation constant (K_I^*, expressed in mole fraction units) of an inhibitor by the relationship (eq A9) in the Appendix:

$$K_I^{eff} = K_I^* \frac{([ND] + K')([ND] + K_d)}{([ND] + K_d^I)} \quad (2)$$

or

$$K_I^{eff} \frac{([ND] + K_d^I)}{([ND] + K_d)} = K_I^* ([ND] + K') \quad (3)$$

where K' is the dissociation constant for the inhibitor bound to the interface (related to the partition coefficient). Identical relations hold for other catalytic-site ligands like substrate or product if I is replaced by S or P, respectively. In special cases the contribution of some of the terms in this equation can be ignored. For example, values of K_I, K^*, and K' for several inhibitors summarized in Table I and II were obtained as follows from the experimentally measured K_I^{eff} values.

(a) By definition, $K_I^{eff} = K_I$ is the effective dissociation constant for EI in the aqueous phase, i.e., [ND] = 0.

(b) When all of the enzyme is in the interface, $K_I^{eff} = K_I^*(K' + [ND])$, and a plot of K_I^{eff} versus [ND] has a slope of K_I^* and the *y*-intercept K_I^*K'. For an inhibitor that is well partitioned in the interface ($K' \ll$ [ND] even at low concentrations of the neutral diluent) the straight line passes through near the origin. This is the behavior of MJ33 in Figure 4, which suggests that this inhibitor was virtually completely partitioned into the micelles of the neutral diluent. In the limit when both enzyme and inhibitor are completely partitioned into the interface, eq 1 can be used directly to get $K_I^{eff} = K_I^*$ if the concentration of inhibitor is expressed as mole fraction in the interface.

(c) According to eq 2, the protection method can also be adopted for situations where the inhibitor has a relatively low affinity for the interface, i.e., poorly partitioned. As shown in Figure 4 for RM-3, the plot of K_I^{eff} versus [ND] has a slope of K_I^* and the *y*-intercept $K'K_I^*$. A relatively large *y*-intercept for RM-3 in Figure 4 suggests that this inhibitor is poorly partitioned into the micelles.

Since the protection experiments are most easily carried out at lower calcium concentrations, the effective dissociation constants have been corrected to apply to saturating calcium by use of eqs A16 and A17 in the Appendix, whose validity has been experimentally demonstrated (Yu et al., 1993). These results show that while the value of K_I^* depends on the polar head-group structure of an inhibitor, it does not change significantly with the increasing chain length. On the other hand, the K' value showed a pronounced dependence on the chain length for the zwitterionic ligands (RM2 versus RM3) and a smaller dependence on the chain length of anionic inhibitors (MJ33 versus MJ72). Although such trends are suggestive, the magnitude of the scatter in the K_I^{eff} values (cf. Figure 4) obtained by the protection method could not be improved further. For example, the two extreme cases shown in Figure 4 provide only the limit estimates for the K' values summarized in Table I. The spectroscopic methods described below confirm the trends and the range of the K_I^* values obtained by the protection method, and the fluorescence method provided values of K' and K_I^* with a significantly lower level of uncertainty.

Table II: Equilibrium Parameters Obtained from the Fluorescence Measurements in 3 mM $CaCl_2$ at pH 8.0 and 24 °C

inhibitor (chain length)	F_{EL}*	K_I^{eff} (μM)	K' (μM/mole fraction)	K_d^I (μM)	K_I* (mole fraction)	K_I (μM)
deoxy-LPC	1.7 (= F_{E*})			900 (= K_d)	>1.8	
MJ33 (16)	3.52	13	<100	20	0.0013	8
MJ72 (8)	3.35	117	300	28	0.002	86
MJ101 (18)	3.53	40	<100	20	0.010	
MJ45 (16)	3.51	42	<100	26	0.009	7.7
MJ102 (14)	3.60	80	<100	22	0.009	
MJ103 (12)	3.53	118	<100	30	0.01	6
MJ104 (10)	3.46	129	150	20	0.013	44
MJ105 (8)	3.35	163	300	40	0.013	62
MG14 (8)	3.5	4.9	1000	28	0.002	40
RM2 (18)	3.34	11	250	65	0.003	
RM3 (8)	3.25	22	4000	151	0.005	70

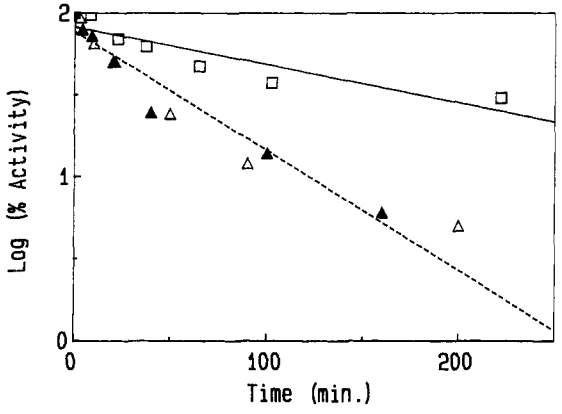

FIGURE 3: Time course of inactivation of PLA2 (0.01 mM in 0.5 mM $CaCl_2$) by *p*-nitrophenacyl bromide (2 mM) (▲) in the presence of 2 mM deoxy-LPC, (△) in the presence of 0.01 mM MJ72, and (□) in the presence of 2 mM deoxy-LPC and 0.01 mM MJ72. In the absence of any additive, the time course of inactivation was the same as with deoxy-LPC (data points not included).

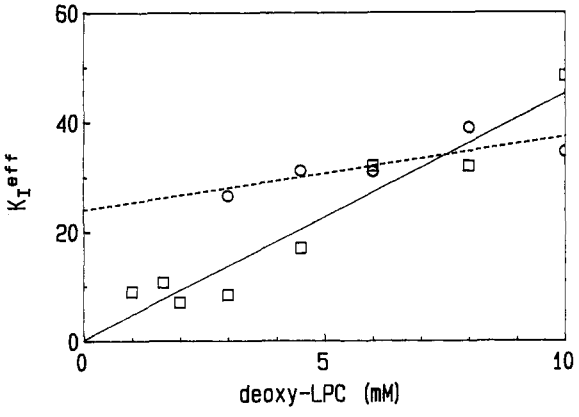

FIGURE 4: Plot of K_I^{eff} versus [ND] for (□) MJ33 and (○) RM-3. The K_I^{eff} values were obtained by the protection method.

Spectroscopic Characterization of the Binding of PLA2 to Micelles of Deoxy-LPC. The spectral perturbations induced on the binding of the enzyme to the interface and those observed on the binding of the active-site-directed ligands to the enzyme at the interface provided a quantitative basis for monitoring such equilibria and obtaining the underlying dissociation constants. Such changes result largely from perturbation of the only tryptophan residue at position 3 of PLA2 (Ramirez & Jain, 1991). The increase in the UV absorbance on the binding of PLA2 to micelles of the neutral diluent (deoxy-LPC) was as a broad peak near 280 nm. On the addition of MJ72 to the mixture of PLA2 and deoxy-LPC, the absorbance increased further, with characteristic well-resolved peaks at 292 and 286 nm. Similar changes were also observed with

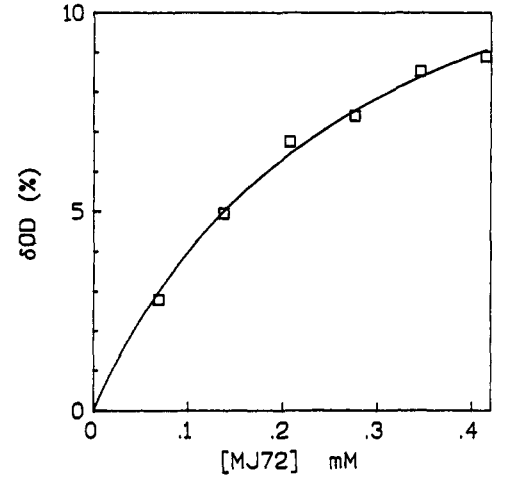

FIGURE 5: Increase in the absorbance at 292 nm as a function of MJ72 concentration added to a mixture of 35 μM PLA2 and 2.2 mM deoxy-LPC.

all the competitive inhibitors, substrate analogs, and the products of hydrolysis added to the neutral diluent. The magnitude of the absorbance change depended upon the concentration of the active-site-directed ligand, and at saturating inhibitor concentration, $\delta\epsilon$ at 292 nm was 2500 cm^{-1} M^{-1}. Such changes in the absorbance were observed only in the presence of calcium and only if the ligand was added in the presence of the neutral diluent. On the other hand, the increase in the absorbance was not observed in the presence of inhibitors dispersed as solitary monomers. Thus the UV absorbance changes shown in the 290-nm region result from the formation of E*I. Additional evidence for this interpretation is reported elsewhere (Jain & Maliwal, 1993).

As shown in Figure 5, the absorbance of PLA2 at 292 nm in deoxy-LPC increased with the concentration of MJ72 added to the reaction mixture. With all the inhibitors tested, the binding isotherms are hyperbolic, and the maximum $\delta\epsilon$ at 292 nm was between 2200 and 2700 cm^{-1} M^{-1}. These binding isotherms were used to calculate values of K_I^{eff}. Since the PLA2 concentration used for these measurements is about 35 μM, the K_I^{eff} values were also corrected for the depletion of the inhibitor, because in the early points of the isotherm the concentration of the free inhibitor may be considerably lower than the total inhibitor concentration. Such corrections were made according to eq A14 given in the Appendix. After such corrections, the K_I^{eff} and K_I* values obtained from the absorbance change (data not shown) were comparable to the values obtained by the protection method (Table I); however, with this method also it was not possible to achieve a significant improvement in the statistical scatter of the primary data. This was probably because the overall increase in the

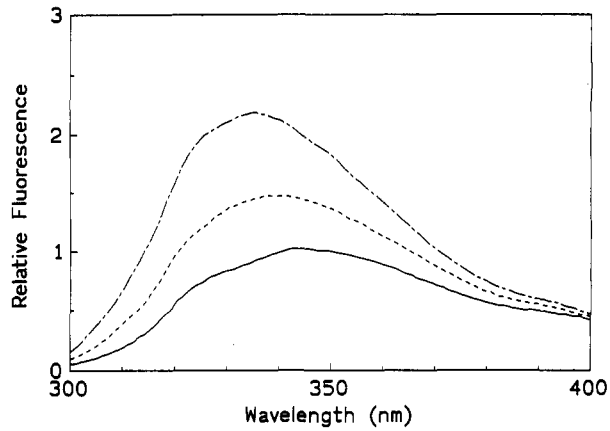

FIGURE 6: Fluorescence emission spectra of PLA2 (2.5 μM) in the aqueous phase (from bottom to top) in the absence of any additive, in the presence of 1.2 mM deoxy-LPC, and in the presence of 1.2 mM deoxy-LPC and 0.17 mM MJ72. At this concentration, MJ72 alone had no noticeable effect on the fluorescence properties of PLA2 in the aqueous phase.

absorbance due to the E*-to-E*L change is relatively small. Also, the UV absorbance method is very sensitive to scattering, as would be expected if the micelle size changes with the concentration of the reactants. For such reasons, this method was not pursued further to quantitatively characterize the E*L dissociation equilibrium. As elaborated next, some of these difficulties were effectively resolved by monitoring the intrinsic fluorescence emission. The overall increase in the fluorescence emission intensity from Trp-3 at 333 nm is more than 250% compared to a change of 40% in the absorbance at 292 nm. The combined facts that the fluorescence changes are relatively insensitive to scattering artifacts and that, in effect, the equilibrium dissociation measurements could be carried out with about 2 μM PLA2 effectively eliminated the need for correction under most experimental conditions used in this study.

Characterization of the Binding of PLA2 by Fluorescence Emission. As shown in Figure 6, the fluorescence emission intensity of PLA2 increased significantly in the presence of deoxy-LPC, and a further increase was observed on the addition of specific ligands such as MJ72. The difference spectra showed that the change in the emission intensity had a maximum at 336 nm, compared to the maximum at 345 nm for the enzyme in the aqueous phase. As developed in the Appendix and outlined below, by monitoring the increase in the fluorescence intensity under appropriate experimental conditions, it was possible to obtain values of several equilibrium dissociation constants defined in Figure 1 and summarized in Table II.

(a) As shown in Figure 7, the increase in the emission intensity at 333 nm showed a hyperbolic dependence on the concentration of deoxy-LPC. The apparent dissociation constant, K_d, for the enzyme bound to micelles of deoxy-LPC was estimated to be 1.6 mM at 3 mM $CaCl_2$. As shown in Figure 7, the deoxy-LPC-mediated fluorescence increase of PLA2 was observed only in the presence of divalent cations such as calcium and cadmium which bind to the active site of the enzyme at the interface, but the change is not observed in the presence of barium, which does not bind to the E* or E*L form of the enzyme (Yu et al., 1993). There is considerable uncertainty in the calculated values of K_d. The binding isotherm shows a systematic deviation when fitted to a single dissociation constant, and the fit shows significant departure at higher concentrations of calcium. From the dependence of K_d on the calcium concentration (results not

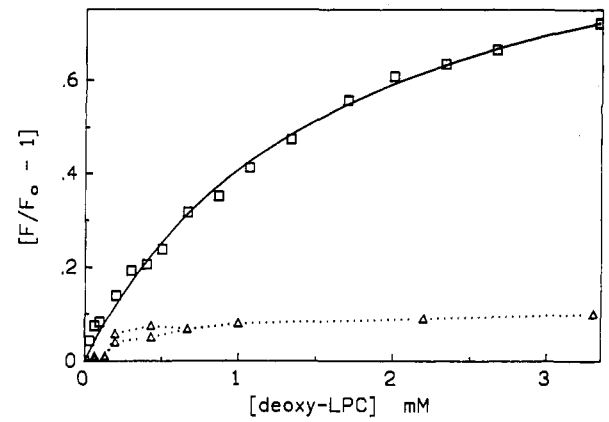

FIGURE 7: Increase in the fluorescence emission from PLA2 at 333 nm as a function of deoxy-LPC concentration in 10 mM Tris·Cl^- and 2.5 μM PLA2 (□) in the presence of 3 mM $CaCl_2$ and (△) in the presence of 0.1 mM EGTA.

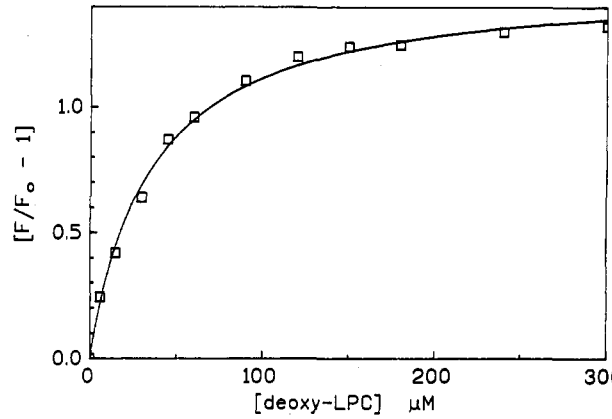

FIGURE 8: Increase in the fluorescence emission intensity at 333 nm as a function of the concentration of MJ33 added to a mixture of 2 μM PLA2 and 3.3 mM deoxy-LPC in the presence of 3 mM calcium and 20 mM Tris at pH 8.0. The theoretical fit for such plots was used to obtain K_I^{eff} values.

shown) it appears that the overall process is considerably more complex, and an attempt is being made to resolve the role of calcium in the E-to-E* equilibrium. It may be noted that such calcium dependence is observed only on zwitterionic micelles because the binding of PLA2 to anionic vesicles is observed even in the absence of calcium.

(b) In the presence of deoxy-LPC and calcium, MJ72 caused a further increase in the fluorescence emission intensity at 333 nm (curve b versus c in Figure 6). Such an increase was observed only in the presence of active-site-directed cations such as calcium and cadmium but not in the presence of barium or EGTA. As summarized in Figure 8, the increase in the fluorescence emission at 3.3 mM deoxy-LPC and 3 mM $CaCl_2$ as a function of the concentration of MJ33 showed a hyperbolic dependence. The K_I^{eff} values calculated from such curves for several inhibitors are summarized in Table II. The maximum relative emission intensity at 333 nm for E* was about 1.7 (= F_{E^*}), compared to the value of 1 for E, whereas for E*L the value was 3.5 (= F_{EL^*}) with several inhibitors.

(c) If a mixture of PLA2 and an inhibitor is titrated with deoxy-LPC, as shown in Figure 9, the increase in the emission intensity shows a hyperbolic dependence. Values of K_d^I from such isotherms were obtained directly if the bulk inhibitor concentration is high enough that all the enzyme in the aqueous phase is in the EI form; otherwise, for appropriate corrections one must use eq A15 developed in the Appendix. The values of K_d^I for several inhibitors obtained by this method are

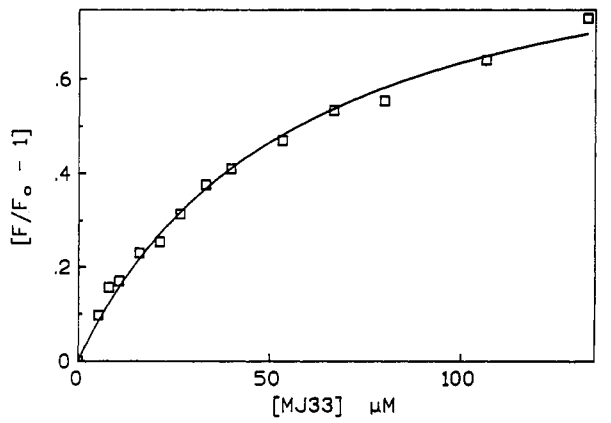

FIGURE 9: Increase in the fluorescence emission intensity at 333 nm as a function of the concentration of deoxy-LPC added to a mixture of 2 μM PLA2, 0.3 mM MJ72, and 3 mM calcium. The theoretical fit for such plots was used to obtained K_d^I values.

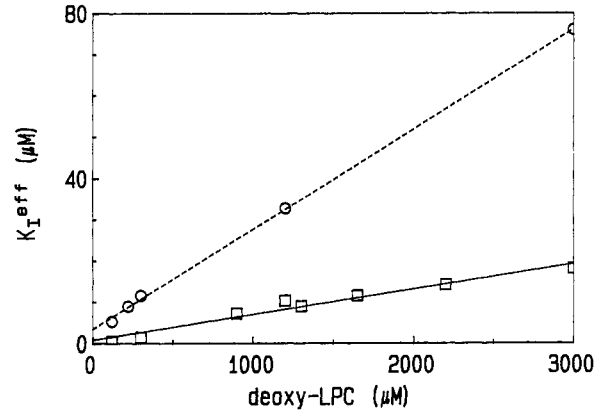

FIGURE 10: Plot of K_I^{eff} versus the concentration of the neutral diluent for (□) MJ33 and (○) MJ72. The K_I^{eff} values were corrected for the neutral diluent concentration according to the left-hand side of eq 3.

summarized in Table II. The K_d^I values are not only considerably smaller than the K_d value, but also they do not appear to depend on the structure of the inhibitor, the concentration of the enzyme, or the concentration of calcium above 1 mM.

Dissection of K_I^{eff} Values. As developed in the Appendix, the K_I^{eff} values obtained from the curves of the type shown in Figure 8 depend on the bulk concentration of the neutral diluent as given by eq 2 or 3. Since the K_d and K_d^I values were determined independently, a plot of the left-hand side of eq 3 as a function of the neutral diluent concentration would give a slope of K_I^* and a y-intercept of $K'K_I^*$. Values of K_I^* and K' obtained from plots of the type shown in Figure 10 are summarized in Table II. The error range in the values of K_I^{eff} measured by these protocols was quite low (probably less than 20%), and therefore the uncertainty in the values of K' is estimated to be less than 50%.

Chain-Length Dependence of K'. Lower K' values (Table II) were obtained for inhibitors with longer alkyl chains. The value of K' for RM-3 is high, and its absolute value is in the range expected for an amphiphile with an octyl chain. The values for anionic MJ72 and MJ105 are considerably smaller than that for zwitterionic RM-3. Since these three inhibitors have only one octyl chain, the difference in their K' values must be due to a difference in their surface charge and possibly due to the overall polarity of the head group. A possible interpretation is that the anionic inhibitors of the MJ series apparently partition better in the PLA2–bilayer complex probably because the interfacial recognition region of PLA2 has a ring of cationic residues (Ramirez & Jain, 1991) which would tend to preferentially sequester anionic amphiphiles at the microinterface of the bound enzyme (E*) and thus effectively reduce the K' value. Detailed significance of this interpretation is being investigated.

DISCUSSION

The differences in the susceptibilities to alkylating agents and the spectroscopic signatures of E, E*, and E*I forms of PLA2 are distinct (Jain & Maliwal 1993). By monitoring such changes, it is possible to determine all the interfacial equilibria involving these species (Figure 1). The formalism, protocols, and conditions and the values of the dissociation constants reported in this paper should be useful in resolving the contributions of the various species present in the interface during interfacial catalysis of PLA2. Specific implications of the methods and results reported in this paper are elaborated below in the context of interfacial catalysis and activation by PLA2.

Methods and Protocols. Each of the three methods used in this study to monitor interfacial equilibria have their windows of advantages and limitations. The protection method is based on the accessibility of His-48; therefore, it is generally applicable to all known secreted PLA2s with histidine at the catalytic site. However, the method is tedious, relatively insensitive, and requires manipulation of the primary data to obtain K_L values (eq 1). On the other hand, the spectroscopic methods take advantage of the perturbation of Trp-3 at the interfacial recognition region which occurs if amphiphiles bind to the interfacial recognition region. Thus a confluence of structural and functional features make Trp-3 an ideal intrinsic probe for the E, E*, and E*L states of pig pancreatic PLA2. In addition, the fluorescence method was well suited for the present study because it required low concentrations of the enzyme; the dynamic range of the signal is over 250%, and the scattering noise and other background changes are negligible.

Binding of PLA2 to aqueous dispersions of a neutral diluent does not protect the active site from alkylation, nor does it cause a characteristic change in the absorbance. About a 100% increase in the fluorescence emission on the binding of PLA2 to micelles of deoxy-LPC is due to the E-to-E* change without any contribution from the E*L species. The fact that a fluorescence change during the E-to-E* transition occurs without the occupancy of the active site was also demonstrated by the observation that alkylated PLA2 showed a 100% increase in the fluorescence emission intensity at 333 nm on binding to the interface (Jain et al., 1991b; Volwerk et al., 1980) without a change in the characteristic absorbance in the 280–300-nm region. The fact that there is no noticeable change in the UV spectrum in the 292-nm region on the binding of PLA2 to micelles of deoxy-LPC suggested that the increase in the fluorescence emission is not due to the presence of an impurity in deoxy-LPC that binds to the active site. This conclusion is further supported by the fact that a similar change in the fluorescence emission without a change in the UV absorbance was also observed in the presence of 2-hexadecylglycerophosphocholine and deoxycholate micelles. It may be noted that a neutral diluent for one particular PLA2 may not necessarily be useful with the enzyme from other sources or the mutants (Bayburt et al., 1993). The criteria and protocols developed here and elsewhere (Jain et al., 1991a,d) to distinguish neutral diluents from active-site-directed inhibitors should, however, be generally applicable.

Significance of the Primary Equilibrium Parameters. The scheme in Figure 1 provides a quantitative basis for structure–activity correlation from which mechanistic and structural information could be obtained. Values of K', the bulk concentration of the interface at which half of the amphiphile is in the interface, were obtained indirectly; however, these values are functionally meaningful since they represent the partitioning of the ligand at the microinterface of the enzyme at the zwitterionic interface. Anomalously low K' values for the short-chain anionic inhibitors are intriguing, i.e., somehow the bound enzyme "sees" a higher concentration of the anionic inhibitors compared to what is expected on the basis of bulk oil–water partition coefficients or to that observed for the zwitterionic inhibitors. These results, therefore, support the notion that the binding of PLA2 to the interface is promoted by the interaction of anionic amphiphiles with a ring of cationic residues at the i-face of PLA2 that is in contact with the bilayer (Ramirez & Jain, 1991). The role of such ionic interactions leading to the high-affinity binding of PLA2 to anionic interface still awaits a detailed molecular description.

Values of K_d^I and K_I^* do not show a significant dependence on the chain length. The hydrophobic effect is apparently not a significant factor in the formation of the E*I complex in the interface. The K_I values change by less than a factor of 10 when the chain length is increased from octyl to hexadecyl (MJ72 and MJ105 versus MJ33 and MJ45 in Tables I and II). These results suggest that the contribution of the hydrophobic effect involving the alkyl chain of the active-site-directed ligand is only a minor factor in the formation of the EI complex. It is possible, although unlikely, that the formation of premicellar aggregates (Rogers et al., 1992) could influences the measured K_I values.

Values of the individual equilibrium dissociation constants also provide insight into the underlying processes. One of the most significant observation summarized in Table II is that the K_d value is about 50-fold larger than the K_d^I values, which are in the 20–80 μM range for the E*I complexes with the various inhibitors. This implies that the alkyl chain length does not contribute to the binding of EI to the interface, i.e., E*I is not anchored via the chain of the bound inhibitor. Why the E*I complex has an effectively lower tendency to dissociate from the zwitterionic micellar interface is not clear. Although it is a possibility, it does not necessarily mean that the enzyme undergoes a conformational change during the EI-to-E*I transition. At this stage we believe that the binding of a ligand to the active site promotes desolvation of the interfacial recognition region, which in turn would induce aggregation of other amphiphiles to the EI complex. The driving force for this process could also come from the reorientation of the amino acid residues in the N-terminus region of PLA2. Spectroscopic results suggest that the E, E*, and E*L forms are not conformationally discrete species but that they represent a range of readily interconvertible conformations, one of which is stabilized in the E*I form (Jain & Maliwal, 1993).

Relationship between the Equilibria. Results show that the binding of PLA2 to the interface can be quantitatively dissected from the binding of an active-site-directed ligand to the enzyme at the interface. According to the "thermodynamic box" shown in Figure 1 and the formalism developed in the Appendix, these constants ultimately relate to the nature of the interactions that stabilize E, E*, EI, and E*I, as well as the distribution of the inhibitor between the interface and the aqueous phase, expressed as K'. Values of the equilibrium dissociation constants summarized in Tables II thus provide a unique opportunity to test the validity of this scheme. The overall consistency of the equilibrium dissociation constants to this cyclic scheme is underscored by the thermodynamic relationship A8 in the Appendix:

$$K'K_dK_I^* = K_IK_d^I \quad (4)$$

The numerical results summarized in Table II for inhibitors are consistent with this relationship to within a factor of 4 if calculated as the ratio K_d/K_d^I, which attests to the validity of the cyclic scheme in Figure 1.

The Equilibrium Parameters Correlate with the Steady-State Kinetic Parameters. The relationship of the interfacial equilibrium constants obtained on micelles of a neutral diluent to the steady-state and equilibrium parameters may also be emphasized. As shown elsewhere, the K_L^* values (for calcium, products, and inhibitors) are entirely consistent with all the steady-state kinetic parameters that describe the progress curve in the scooting mode on bilayer vesicles of anionic phospholipids in the presence or absence of a neutral diluent (Berg et al., 1991; Jain et al., 1993), the kinetics of inhibition (Jain et al., 1991a,d), and the obligatory requirement of calcium for the binding of active-site-directed ligands and for catalysis (Yu et al., 1993). Such a quantitative correspondence between the equilibrium measurements on micelles and the steady-state kinetic measurements on vesicles shows that the intrinsic properties of the enzyme bound to such diverse interfaces are virtually the same within the resolution of the methods used for such studies.

Kinetic Basis of Interfacial Activation. The term interfacial activation often refers to the enhanced rate of catalysis observed with substrate present at the lipid–water interface compared to that for the same substrate present as solitary monomers in solution (de Haas et al., 1971; Pieterson et al., 1974). Several classes of membrane-bound enzymes (Jain & Zakim, 1987), including β-hydroxybutyrate dehydrogenase (Fleischer et al., 1983), show activity only when reconstituted at the interface. Such cases cannot, however, be taken as examples of interfacial activation because these enzymes may be denatured in the absence of the interface and therefore catalytically inactive. Although this is not the case for PLA2, in spite of numerous suggestions about interfacial activation of PLA2 (Verger & de Haas, 1976; Volwerk & de Haas, 1982; Dennis, 1983), no consensus has emerged on the underlying mechanism, largely because a rigorous interpretation of the results of the kinetics of interfacial catalysis in terms of the underlying kinetic and equilibrium parameters has not been possible until recently (Jain & Berg, 1989; Berg et al., 1991). Within the context of the kinetic scheme for interfacial catalysis, several possibilities may be considered to account for interfacial activation; as follow.

(a) Binding of the enzyme from the aqueous phase to the interface makes the substrate accessible for the catalytic turnover by the bound enzyme. Such effects increase the observed rates of hydrolysis by phospholipase A_2 by several orders of magnitude in the presence of suitable additives (Jain et al., 1982, 1986a,b; Ghomashchi et al., 1991). For example, the value of K_d on the zwitterionic interface is considerably larger than that observed on the anionic interfaces.

(b) If the intrinsic rate of catalytic turnover is large, then the rate of hydrolysis of substrate present in small aggregates becomes limited by the rate of replenishment of the substrate, i.e., the steady-state condition is not satisfied on the microscopic level (Jain et al., 1991a,c, 1992, 1993). Thus in mixed micelles the chemical step is not rate-limiting due to a decrease in the size of the substrate dispersions where the rate of

replenishment of the substrate could become rate-limiting (Jain et al., 1993).

(c) A consideration of interfacial activation in terms of a possible difference in the conformation of the substrate in the aqueous phase versus interface can be ruled out on the basis of the results that show that the conformations of phospholipid molecules at the interface and in solutions are virtually the same as in crystals (Hauser et al., 1981). Similarly, the energy differences and the rate barriers for the conformers present at the active site are probably insignificant compared to the activation energy for any of the steps explicitly considered for the catalytic turnover cycle.

(d) It has been argued that the local concentration (number density) of the substrate in the interface is high, which would favor the formation of the E*S complex rather than the formation of the ES complex. On the basis of the microscopic reversibility of these two steps, it can be argued that a local concentration effect as such will not effectively increase the overall substrate binding to the active site because the apparent affinity of the substrate for the interface (which increases the local concentration in the interface through the partitioning) will also (probably to the same extent) reduce the binding of the substrate to the enzyme at the interface. Other variations on this theme are elaborated next.

(e) Considerations related to the partitioning and higher local concentration of the substrate that the bound enzyme "sees" at the interface deserve further elaboration in terms of the equilibria in Figure 1. In solution, the enzyme has the dissociation constant K_I relative to the free concentration of inhibitor. Similarly, the local concentration that the surface-bound enzyme "sees" is $X_I[ND]_m = [I]_T[ND]_m/(1 + [ND]_T/K')$. In terms of this local concentration of the inhibitor, the dissociation constant for the surface-bound enzyme is

$$K^*_{I,local} = K_I \frac{K_d^I}{K_d} \frac{[ND]_m}{K'} = K_I \frac{K_d^I}{K_d} P_I \qquad (5)$$

where the partition coefficient, P_I, for the inhibitor into the membranes has been introduced. This effective local dissociation constant is, in fact, much larger than K_I so that localization in the membrane actually decreases binding if the relations are normalized to the same local inhibitor concentration.

(f) Equation 5 can be dissected further to elaborate on certain other possibilities. The factor P_I, if larger than 1, accounts for the fact that the inhibitor "likes" its surroundings in the membrane better than in solution. This increases not only its concentration in the membrane but also the difficulty of pulling it into the catalytic site. These two effects compensate each other in the overall effective binding constant of eq A9. Therefore, the interfacial activation factor K_d^I/K_d (eq 5) may be interpreted as an "anchoring effect", implying that the inhibitor-bound enzyme sticks better to the interface ($K_d^I < K_d$, as observed). In the simplest picture, the enzyme-bound ligand has a tail that sticks out and interacts with the membrane; this tail would then serve to anchor the enzyme to the interface, but it would also mean that the whole inhibitor would not have to be pulled out of the membrane to bind the enzyme, thereby reducing the effect of the large P_I. If this is the case, then the apparent increased inhibitor bindng to the surface-associated enzyme would not be caused by an "activation of the enzyme" but rather by the changed environment of the inhibitor. The difficulty with this interpretation of the activation factor is that it predicts that the factor K_d^I/K_d would be sensitive to the chain length of the inhibitor. Results summarized in Table II show that this is not the case.

Having ruled out the physical and substrate-based mechanisms, we seek the basis for interfacial activation in the primary kinetic and equilibrium properties of the enzyme such as the allosteric modulation of the enzyme on the binding to the interface. According to the formalism of allosteric activation (York, 1992), the K_M (K-) and k_{cat} (V-) type of activation are distinguished. Since the rate of hydrolysis of "soluble" substrates (such as short-chain diacylphosphatidylcholines dispersed below their critical micelle concentrations) does not significantly change in the presence of the dispersions of neutral diluents (M. K. Jain et al., unpublished observations), it may be argued that the k_{cat} type of interfacial activation does not occur on the binding of PLA2 to the interface. On the other hand, results in Tables I and II show that $K_I > K_I^{eff}$, i.e., the apparent affinity is higher in the presence of the interface of the neutral diluent. Similar differences were noted in the I(50) values obtained by monitoring the kinetics of inhibition (Yuan et al., 1990; de Haas et al., 1971) and the K_I^* values under the kinetic conditions (Rogers et al., 1992). Such results suggest that interfacial activation of pig pancreatic phospholipase A_2 is of K_M type, i.e., the affinity of the enzyme for the active-site-directed ligands is altered on the binding of the enzyme to the interface. In this context we consider the results for the inhibitor binding to be representative also of the properties of the substrate binding at the catalytic site.

The effective dissociation constant for the inhibitor in terms of the overall concentrations, eq A9, decreases with increasing interface except when $[ND]_T > K'$, in which case dilution effects start to dominate. At saturating interface, the effective dissociation constant is decreased by the factor K_d^I/K_d if the dilution effect is disregarded. Thus, in terms of the overall concentrations, there is an apparent activation of the surface-associated enzyme by the factor K_d/K_d^I. Obviously, the factor K_d^I/K_d could be due to a change in the state of the enzyme when the inhibitor binds. If inhibitor in this way increases the interface binding to the enzyme, the interface must also increase the inhibitor binding by the same factor. Thus it is possible that the interface activates the pig pancreatic PLA2 by a factor K_d/K_d^I, which at saturating calcium would be about 50-fold for most of the active-site-directed ligands including the substrate and inhibitors.

To recapitulate, the kinetic and equilibrium behavior of PLA2 is entirely consistent with not only the two-stage adaptation of the Michaelis–Menten formalism for interfacial catalysis but also the thermodynamic cycle shown in Figure 1. The results show that the intrinsic interfacial equilibria involving PLA2 are virtually the same in micelles of zwitterionic neutral diluents or on vesicles of anionic phospholipids. The fact that interfacial activation can be accommodated within this framework of the Michaelis–Menten formalism adopted for the interface suggests that the primary rate and equilibrium parameters provide a meaningful basis for the structure–function correlation for lipolytic enzymes. The structural basis for interfacial activation is yet to be elaborated. Although it has been suggested that the binding of the enzyme to the interface causes a discrete conformational change (Volwerk & de Haas, 1982), at this stage we prefer the possibility that the enzyme in the aqueous phase exists as an ensemble of readily interconvertible conformations, only one of which is stabilized on the binding of a ligand to the active site ("induced fit"). The role of the N-terminus segment and

the desolvation of the active site and the interfacial recognition region in the stabilization of the E* and E*I forms of PLA2 are being investigated.

APPENDIX

Interfacial Equilibria. The experiments described in the main text require us to consider at least three coupled binding equilibria for PLA2: binding to the interface and the catalytic-site binding of calcium and inhibitor. Some of these binding reactions interact strongly. Thus, binding of calcium at the catalytic site is required before inhibitor can bind there. On the other hand, interface binding seems to have only a small influence on the calcium binding at the catalytic site; therefore, interface binding must also be fairly independent of the catalytic calcium binding. These results considerably simplify the overall reaction scheme which can be described in a 3 × 2 state diagram for the enzyme: From left to right, the scheme

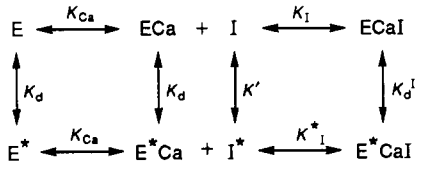

(A1)

implies first binding of a calcium ion at the catalytic site (E to ECa with dissociation constant K_{Ca}) and then binding of inhibitor. From top to bottom, the scheme implies enzyme binding to the interface (E to E* with dissociation constant K_d in the absence of inhibitor and K_d^I in its presence).

Saturating Calcium. When binding of calcium at the catalytic site is saturated ([Ca] $\gg K_{Ca}$), the leftmost column in the scheme above disappears, and the scheme is effectively reduced to where for convenience the bound calcium ion has

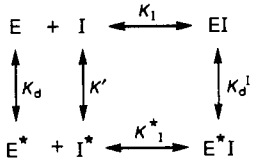

(A2)

been left out in the notation of the various enzyme complexes.

Since the equilibria involve both bulk solution and interface, some care has to be taken in the choice of units for concentrations and equilibrium constants. In the following, quantities with an asterisk refer to the interface, while concentrations counted as moles per volume of aqueous phase have a subscripted w. Thus, for instance, $[I^*]_w$ refers to the moles of inhibitor in the interface counted per unit volume of the water phase.

The various equilibrium constants in the scheme A2 can be defined as follows. First, the partition of the inhibitor between the water phase and the membrane phase is defined by

$$K' = [I]_w[ND^*]_w/[I^*]_w = [I]_w\left(\frac{1}{X_I^*} - 1\right) \approx [I]_w/X_I^* \quad \text{(A3)}$$

where ND* refers to the amount of membrane-forming amphiphile (neutral diluent) that is in the water interface of the membranes and X_I^* is the mole fraction of inhibitor in the interface. The approximation in (A3) holds as long as X_I^* is small. The equilibrium constant K' is related to the partition coefficient for the inhibitor, P_I, as $P_I = [I]_m/[I]_w = X_I[ND]_m/[I]_w = [ND]_m/K'$. Here, the subscript m denotes the concentration counted as moles per unit volume of the membrane phase, and the last equality follows if the mole fraction of inhibitor is the same throughout the membrane phase, $X_I = X_I^*$. Note the difference between ND* and ND, where ND is the total amount of neutral diluent in the membranes and ND* is the amount in the membranes facing the water, e.g., for vesicles only the outer membrane can be considered part of the interface, ND*, and ND*/ND is approximately 0.5. For micelles, as in this study, there is no difference between ND and ND*.

The enzyme and the enzyme–inhibitor complex bind to the interface with the following dissociation constants

$$K_d = [ND^*]_w[E]_w/[E^*]_w \quad \text{(A4)}$$

$$K_d^I = [ND^*]_w[EI]_w/[E^*I]_w \quad \text{(A5)}$$

These relations hold as long as the bound enzymes do not cover a significant fraction of the interface, thereby reducing available surface sites. (Alternatively, $[ND^*]_w$ in these equations must be considered as the concentration of interface not covered by enzyme.) The dissociation constants for the enzyme–inhibitor complex in solution and in the interface can be written as

$$K_I = [E]_w[I]_w/[EI]_w \quad \text{(A6)}$$

$$K_I^* = [E^*]_w X_I^*/[E^*I]_w \quad \text{(A7)}$$

These equilibrium constants are not all independent but are related through a thermodynamic relationship:

$$K_d^I/K_d = K'K_I^*/K_I \quad \text{(A8)}$$

This can easily be shown to hold using the definitions above, eqs A3–A7.

An effective dissociation constant for the enzyme–inhibitor complex can be defined by considering the amounts of complexes, free enzyme, and free inhibitor irrespective of whether they are in the membrane, in the interface, or in bulk solution. If concentrations per total volume (water phase plus membrane phase) are denoted by subscript T, then we can define

$$K_I^{eff} = \frac{[I + I_m]_T[E + E^*]_w}{[EI + E^*I]_w} = K_I^*[ND]_T\frac{(1 + f_wK'/[ND]_T)(1 + K_d/[ND^*]_w)}{(1 + K_d^I/[ND^*]_w)}$$

$$= K_I(1 + [ND]_T/K')\frac{(1 + [ND^*]_w/K_d)}{(1 + [ND^*]_w/K_d^I)} \quad \text{(A9)}$$

In the second equality, the fraction, f_w, of the total volume that is aqueous has been introduced; this fraction is close to 1 under most experimental conditions (and in this study) and has been dropped in what follows. $[ND]_T$ denotes the concentration of neutral diluent in the membranes counted per unit of total volume; the amount of free neutral diluent in water solution, on the other hand, is assumed small. Under conditions where all the enzyme is in the interface, eq A9 reduces to

$$K_I^{eff} = K_I^*(K' + [ND]_T) \quad \text{(A10)}$$

This is a particularly useful limit for determining K' and K_I^*, where a plot of K_I^{eff} versus $[ND]_T$ gives a straight line with slope K_I^* and intercept $K'K_I^*$. If all the enzyme is not in the

interface, eq A9 can be rearranged to give

$$K_I^{eff}(K_d^I + [ND^*]_w)/(K_d + [ND^*]_w) = K_I^*(K' + [ND]_T) \quad (A11)$$

Thus, if K_d and K_d^I have been determined independently, the measured K_I^{eff} values can be adjusted according to the left-hand side of eq A11 to give the same straight-line relationship as in eq A10.

The effective dissociation constant, K_I^{eff}, defined above is the one that will be measured in experiments that monitor only the fraction of enzyme that is in enzyme–inhibitor complexes, regardless of whether the enzyme is in the interface or in bulk solution. This gives the simple hyperbolic binding curve for enzyme–inhibitor complex as a function of free inhibitor concentration. K_I^{eff} will be most easily measured under conditions where inhibitor is in large excess over enzyme so that the amount of free inhibitor is the same as the total added. If inhibitor is not in large excess over enzyme, then the usual quadratic relationship involving the total inhibitor concentration must be used, eq 2 of the main text. From the equilibria in the scheme A2, this relation can be derived as follows. If f denotes the fraction of enzyme that is in complex with inhibitor, one finds

$$f = \left(\frac{[I]_w}{K_I} + \frac{X_I[ND^*]_w}{K_I^* K_d}\right) \Big/ \left[1 + \frac{[I]_w}{K_I} + \frac{X_I}{K_I^*}\left(1 + \frac{[ND^*]_w}{K_d}\right)\right]$$

$$= \frac{[I]_w(1 + [ND^*]_w/K')}{[I]_w(1 + [ND^*]_w/K') + K_I^{eff}} \quad (A12)$$

In the last equality, eq A3 has been used to eliminate X_I and K_I^{eff} from eq A9 has been entered. Furthermore, the concentration of the total amount of added inhibitor is

$$[I_T]_w = [I]_w + [ND]_w X_I + [E_T]_w f = [I]_w(1 + [ND^*]_w/K') + [E_T]_w f \quad (A13)$$

where the term $[E_T]_w f$ is the concentration of EI and E*I complexes. Using eqs A12–A13 to eliminate $[I]_w$, one finds

$$K_I^{eff} f = (1 - f)([I_T]_w - [E_T]_w f) \quad (A14)$$

Since the addition of inhibitor can also shift the E-to-E* equilibrium, eq A14 is valid only in the limits when saturation effects do not affect this equilibrium. This holds only under conditions where all enzyme is bound at the interface or when interface sites are in large excess over enzyme.

In the same way, one can define an effective dissociation constant for the enzyme and the interface:

$$K_d^{eff} = \frac{[ND^*]_w[E + EI]_w}{[E^* + E^*I]_w} = K_d \frac{1 + [ND]_T/K' + [I]_T/K_I}{1 + [ND]_T/K' + [I]_T/(K'K_I^*)} \quad (A15)$$

This is the effective dissociation constant at any particular concentration $[ND]_T$. However, in a titration with ND, it is not a proper constant except in the limits of very small or very large concentrations of inhibitor or when $[ND]_T \ll K'$.

Calcium Dependence. Inhibitor binding by the protection experiments must be measured below the saturation limit for calcium. The interface binding is more conveniently studied at higher calcium concentrations. Thus, one needs to consider the calcium dependence in order to set these results in relation to each other. Equations A3–A15 above could be used to describe the inhibitor and interface binding states of the enzyme at any one particular concentration of calcium, even if it is not saturating. In this case, the various dissociation constants would have to be replaced by effective calcium-dependent quantities. Using the full 2 × 3 scheme above, (A1), one finds that the Ca-saturated dissociation constants K_I and K_I^* in the relations A6–A15 above should be replaced by the calcium-dependent quantities

$$K_I(Ca) = K_I(1 + K_{Ca}/[Ca]) \quad (A16)$$

$$K_I^*(Ca) = K_I^*(1 + K_{Ca}/[Ca]) \quad (A17)$$

The results are based on the assumption that the partitioning of the inhibitor into the membranes does not depend on calcium. These calcium-dependent quantities also satisfy the thermodynamic relationship, eq A8, as do the calcium-saturated ones. Experimental verification of these relations is given in Yu et al. (1993).

REFERENCES

Bayburt, T., Yu, B.-Z., Lin, H. K., Browning, J., Jain, M. K., & Gelb, M. H. (1993) *Biochemistry 32*, 573–582.

Berg, O. G., Yu, B.-Z., Rogers, J., & Jain, M. K. (1991) *Biochemistry 30*, 7283–7297.

de Haas, G. H., Bonsen, P. P. M., Pieterson, W. A., & van Deenen, L. L. M. (1971) *Biochim. Biophys. Acta 239*, 252–266.

Dennis, E. A. (1983) in *The Enzymes*, Vol. 16, pp 307–353, Academic Press, New York.

Fleischer, S., McIntyre, J. O., Churchill, P., Fleer, E., & Maurer, A. (1983), in *Structure and Function of Membrane Proteins* (Quagliarielli, E., & Palmieri, E., Eds.) pp 283–300, Elsevier, Amsterdam.

Ghomashchi, F., Yu, B.-Z., Berg, O. G., Jain, M. K., & Gelb, M. H. (1991) *Biochemistry 30*, 7318–7329.

Hauser, H., Pascher, I., Pearson, R. H., & Sundell (1981) *Biochim. Biophys. Acta 650*, 21–51.

Hille, J. D. R., Egmond, M. R., Dijkman, R., van Oort, M. G., Jirgensons, B., & de Haas, G. H. (1983) *Biochemistry 22*, 5347–5353.

Jain, M. K., & Zakim, D. (1987) *Biochim. Biophys. Acta 906*, 33–68.

Jain, M. K., & Berg, O. G. (1989) *Biochim. Biophys. Acta 1002*, 127–156.

Jain, M. K., & Rogers, J. (1989) *Biochim. Biophys. Acta 1003*, 92–97.

Jain, M. K., & Maliwal, B. P. (1993) *Biochemistry*, in press.

Jain, M. K., Egmond, M. R., Verheij, H. M., Apitz-Castro, R. J., Dijkman, R., & de Haas, G. H. (1982) *Biochim. Biophys. Acta 688*, 341–348.

Jain, M. K., Rogers, J., Jahagirdar, D. V., Marecek, J. F., & Ramirez, F. (1986a) *Biochim. Biophys. Acta 860*, 435–447.

Jain, M. K., Rogers, J., Marecek, J. F., Ramirez, F., & Eibl, H. (1986b) *Biochim. Biophys. Acta 860*, 462–474.

Jain, M. K., Yuan, W., & Gelb, M. H. (1989) *Biochemistry 28*, 4135–4139.

Jain, M. K., Yu, B.-Z., Rogers, J., Ranadive, G. N., & Berg, O. G. (1991a) *Biochemistry 30*, 7306–7317.

Jain, M. K., Ranadive, G., Yu, B.-Z., & Verheij, H. M. (1991b) *Biochemistry 30*, 7330–7140.

Jain, M. K., Rogers, J., Berg, O., & Gelb, M. H. (1991c) *Biochemistry 30*, 7340–7348.

Jain, M. K., Tao, W., Rogers, J., Arenson, C., Eibl, H., & Yu, B.-Z. (1991d) *Biochemistry 30*, 10256–10268.

Jain, M. K., Yu, B. Z., Rogers, J., Gelb, M. H., Tsai, M. D., Hendrickson, E. K., & Hendrickson, H. S. (1992) *Biochemistry 31*, 7841–7847.

Jain, M. K., Rogers, J., Hendrickson, H. S., & Berg, O. G. (1993) *Biochemistry 32*, 8360–8367.

Niewenhuizen, W., Kunze, H., & de Haas, G. H. (1974) *Methods Enzymol. 32B*, 147–154.

Peters, A. R., Dekker, N., Van den Berg, L., Boelens, R., Kaptein, R., Slotboom, A. J., & de Haas, G. H. (1992) *Biochemistry 31*, 10024–10030.

Pieterson, W. A., Vidal, J. C., Volwerk, J. J., & de Haas, G. H. (1974) *Biochemistry 13*, 1455–1460.
Radvanyi, F., Jordan, L., Russo-Marie, F., & Bon, C. (1989) *Anal. Biochem. 177*, 103–109.
Ramirez, F., & Jain, M. K. (1991) *Protein 9*, 229–239.
Rogers, J., Yu, B.-Z., & Jain, M. K. (1992) *Biochemistry 31*, 6056–6062.
Scott, D. L., White, S. P., Otwinowski, Z., Yuan, W., Gelb, M. H., & Sigler, P. B. (1990) *Science 250*, 1541–1546.
Segel, I. H. (1976) in *Enzyme Kinetics*, Wiley, New York.
Slotboom, A. J., Jensen, E. H. J. M., Vlijm, H., Pattus, F., Soares de Araujo, P., & de Haas, G. H. (1978) *Biochemistry 17*, 4593–4600.
Thunnisen, M. M. G. M., Eiso, A. B., Kalk, K. H., Drenth, J., Dijkstra, B. W., Kuipers, O. P., Dijkman, R., de Haas, G. H., & Verheij, H. M. (1990) *Nature 347*, 689–691.
van den Bergh, C. J., Bekkers, C. A. P. A., Verheij, H. M., & de Haas, G. H. (1989) *Eur. J. Biochem. 182*, 307–313.
Van Eijk, J. H., Verheij, H. M., Dijkman, R., & de Haas, G. H. (1983) *Eur. J. Biochem. 132*, 183–188.
Van Oort, M. G., Dijkman, R., Hille, J. D. R., & de Haas, G. H. (1985) *Biochemistry 24*, 7987–93; 7993–99.
Verger, R., & de Haas, G. H. (1976) *Annu. Rev. Biophys. Bioeng. 5*, 77–117.
Verheij, H. M., Slotboom, A. J., & de Haas, G. H. (1981) *Rev. Physiol. Biochem. Pharmacol. 91*, 91–203.
Volwerk, J. J., & de Haas, G. H. (1982) in *Lipid-Protein Interactions 1* (Jost, P. C., & Griffith, O. H., Eds.) pp 69–149, Wiley, New York.
York, J. L. (1992) in *Textbook of Biochemistry* (Devlin, T. M., Ed.) pp 135–193, Wiley, New York.
Yu, B.-Z., Berg, O. C., & Jain, M. K. (1993) *Biochemistry 32*, 6485–6492.
Yuan, W., Quinn, D. M., Sigler, P. B., & Gelb, M. H. (1990) *Biochemistry 29*, 6082–6094.